

LOW TEMPERATURE CATALYTIC OXIDATION OF CHLOROBENZENE OVER $\text{MnO}_x/\text{TiO}_2$ -CNTs NANO-COMPOSITES PREPARED BY WET SYNTHESIS METHODS

Wei Tian, Hangsheng Yang, Xiaoyu Fan, Xiaobin Zhang
State Key Laboratory of Silicon Materials, Department of Materials Science and Engineering, Zhejiang University, Zheda Road 38, Hangzhou 310027, China

1. Introduction

The word “dioxins” collectively refers to a group of stable compounds consisting of three aromatic cycles [1]. Dioxins are among the most toxic Cl-VOCs compounds, which are formed in many kinds of combustion processes of organic fuels in the presence of chlorinated compounds.

To date, the catalytic oxidation of Cl-VOCs to carbon dioxide, HCl, and water is the best method for their destruction. Noble metals [2, 3], perovskites [4, 5] and transition metal oxide-based catalysts [6] constitute the major class of catalysts. Noble metal-based catalysts suffer, however, from the severe deactivation in the presence of Cl [7, 8]. Also, perovskites only show good activity at reaction temperatures above 500 °C. Recently it was reported that some transition metal oxides, especially manganese oxides, were promising candidates to catalyze the Cl-VOCs at reduced temperature [9, 10].

In a recent review, attention has also been paid to the fact that carbon nanotubes (CNTs) are attractive and competitive catalyst supports when compared to activated carbon, due to their electronic, mechanical and thermal properties [11]. CNTs are also found to be superior adsorbent of dioxins [12] and aromatics [13]. For example, the amount of dioxins adsorbed on CNTs is suggested to be 10^{34} higher than those on activated carbon (ZX-4 carbon) [12]. Some recent studies have emphasized the preparation of new hybrid materials CNTs– TiO_2 [14, 15]. In this abstract, $\text{MnO}_x/\text{TiO}_2$ -CNTs composites were prepared and their properties for the promotion of catalytic oxidation of CB, a substitute molecule of dioxins normally used in the laboratory, were investigated.

2. Materials and methods

2.1. Catalysts preparation

For solvothermal method (St), tetrabutyl titanate (0.1 mol) and acetic acid were dissolved in ethanol (200 mL). Manganese nitrate (0.01 mol), ethanol (20 mL), deionized water (8 mL), and nitric acid (3 mL) were mixed and then introduced into the ethanolic solution of tetrabutyl titanate. Then, purified CNTs [16] were dispersed in ethanol, and dropped into the above mixture under sonication. Finally, the mixture was transferred into Teflon-steel autoclave, maintained at 230 °C for 2.5 h. The sample was separated by filtration, washed with deionized water until neutral pH of the washing solution, and finally dried in an oven at 100 °C for 4 h to obtain MnO_x (10 wt%)/ TiO_2 -CNTs (10 wt%) composite catalyst.

For sol-gel method (Sg), tetrabutyl titanate (0.1 mol) and acetic acid were dissolved in ethanol (100 mL). Manganese nitrate (0.01 mol), ethanol (20 mL), deionized water (8 mL), and nitric acid (3 mL) were mixed and then dropped into the ethanolic solution of tetrabutyl titanate under sonication until a yellow transparent sol was formed. Then, purified CNTs dispersed in ethanol were introduced into the sol under vigorous stirring. The mixture was kept stirring until the form of a homogenous CNTs-contained gel. The gel was dried using freeze drying method, resulting in xerogel. The obtained xerogel was crushed into fine powder, and then calcined at 500 °C in a flow of N_2 for 6 h to obtain MnO_x (10 wt%)/ TiO_2 -CNTs (10 wt%) composite catalyst.

For comparison, we also prepared samples of MnO_x (20 wt%)/ TiO_2 without CNTs by the

above-mentioned methods and MnO_x (10 wt%)/CNTs by wet synthesis method [17].

2.2. Characterization and measurements

The catalytic properties of the catalysts were characterized in a fixed-bed flow reactor, in which catalysts were placed in stainless steel tubes with an inner diameter of 1 cm. The experiments were performed under atmospheric pressure at 150–300 °C. Amount of 3 g catalysts was placed at the bed of the reactor. The total gas flow rate passing through the reactor was set at 3000 sccm, corresponding to a gas hour space velocity (GHSV) of 36000 h^{-1} . The CB-containing feed stream to the reactor was carried by argon and controlled by a mass flow controller. The concentration of CB in the reactor feed was set at 100 ppm. Effluent gases were analyzed at a given temperature using an online gas chromatographer (GC 9790).

3. Results and discussion

3.1. XRD, SEM and TEM analysis

Fig. 1 shows the XRD spectra of $\text{MnO}_x/\text{TiO}_2$ -CNTs and $\text{MnO}_x/\text{TiO}_2$ composites. From curves a and b, only peaks attributed to anatase TiO_2 were observed. The (002) reflection at 26.4° from CNTs were overlapped by the anatase (101) reflection at 25.3° [15]. No visible MnO_x peaks can be observed in the XRD spectra, which may be due to the good dispersion of manganese oxide monolayer on the binary support [18, 19]. From curve c of the $\text{MnO}_x/\text{TiO}_2$ (St), TiO_2 existed also in anatase phase, and peaks attributed to MnTiO_3 were detected possibly because of high temperature and high pressure of St which enabled the formation of solid solution between TiO_2 and MnO_x . From curve d of $\text{MnO}_x/\text{TiO}_2$ (Sg), besides the peaks of anatase TiO_2 , several new peaks assigned to the rutile phase were also observed. Moreover, several small peaks attributed to Mn_2O_3 were also detected.

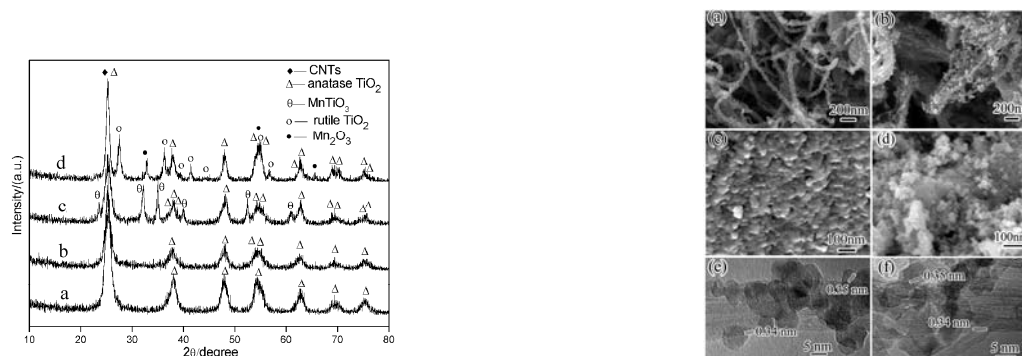


Fig.1 XRD patterns of (a) $\text{MnO}_x/\text{TiO}_2$ -CNTs (St), (b) $\text{MnO}_x/\text{TiO}_2$ -CNTs (Sg), (c) $\text{MnO}_x/\text{TiO}_2$ (St), and (d) $\text{MnO}_x/\text{TiO}_2$ (Sg). (Left one)

Fig.2 SEM and TEM images of catalysts; (a) $\text{MnO}_x/\text{TiO}_2$ -CNTs (St); (b) $\text{MnO}_x/\text{TiO}_2$ -CNTs (Sg); (c) $\text{MnO}_x/\text{TiO}_2$ (St); (d) $\text{MnO}_x/\text{TiO}_2$ (Sg); (e) TEM images of $\text{MnO}_x/\text{TiO}_2$ -CNTs (St); and (f) TEM images of $\text{MnO}_x/\text{TiO}_2$ -CNTs (Sg). (Right one)

Fig. 2 shows typical SEM and TEM images of $\text{MnO}_x/\text{TiO}_2$ and $\text{MnO}_x/\text{TiO}_2$ -CNTs composites. For the composite prepared by St as shown in Fig. 2a, a smooth, uniform coating of CNTs by $\text{MnO}_x/\text{TiO}_2$ nanoparticles was observed; the grain sizes of $\text{MnO}_x/\text{TiO}_2$ were smaller than 10 nm. For the composite prepared by Sg as shown in Fig. 2b, though the aggregation of CNTs in bundles due to van der Waals interaction was still observed [20], the CNTs were also uniformly coated with very small $\text{MnO}_x/\text{TiO}_2$ nanoparticles. Figs. 2c and 2d show the $\text{MnO}_x/\text{TiO}_2$ without CNTs, in which their grain size was much bigger than those observed in Figs. 2a and 2b. Figs. 2e and 2f show the TEM images of composites with CNTs, part of the CNTs surface was coated by small $\text{MnO}_x/\text{TiO}_2$ particles with a grain size approximately 5 nm. And the lattice spacing of nano-particles in both composites was determined to be 0.35 nm, corresponding to the (101) plane of anatase phase [21]. No MnO_x particles were observed by

evaluation of the lattice spacing in all of our TEM observations, suggesting the possibility of the formation of amorphous MnO_x .

3.3. TPR analysis

Fig. 3 shows the TPR profiles of the catalysts and purified CNTs. In TPR curve of purified CNTs, there is only one main peak between 500-750 °C, corresponding to the reaction between H_2 and the -C-O, -COO groups which brought by HNO_3 during purification process on the surface of purified CNTs [15]. For all the catalysts except $\text{MnO}_x/\text{TiO}_2$ (St), TPR curves showed three main peaks, corresponding to the reduction of MnO_2 to Mn_2O_3 , Mn_2O_3 to Mn_3O_4 , and Mn_3O_4 to MnO , respectively [22-24]. The last peak at 500 °C in the $\text{MnO}_x/\text{TiO}_2$ -CNTs (St) may correspond to the reaction between H_2 and the functional groups on CNTs. In the profile of $\text{MnO}_x/\text{TiO}_2$ (St) there is only one main peak, possibly corresponding to the reaction of Mn^{3+} to Mn^{2+} . Moreover, the reaction temperatures of all reduction peaks for catalysts $\text{MnO}_x/\text{TiO}_2$ -CNTs were at least 50 °C lower than those for $\text{MnO}_x/\text{TiO}_2$, suggesting that the CNTs-containing catalysts have better oxidation ability in a lower temperature region, thus higher catalytic activity.

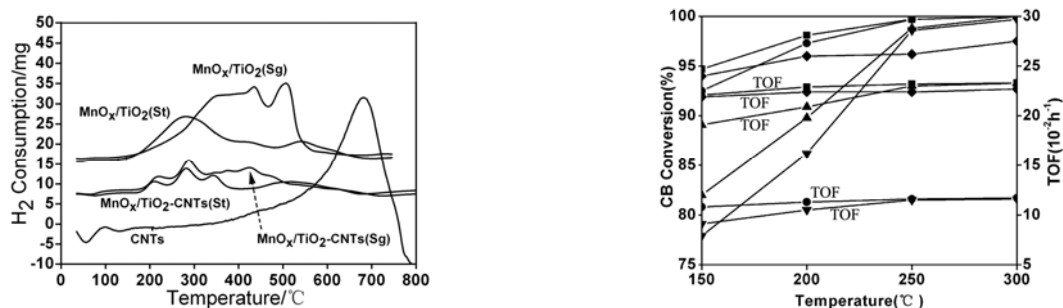


Fig.3 TPR profiles of the catalysts and purified CNTs. (Left one)

Fig. 4 CB conversion activity and TOF of the catalysts: $\text{MnO}_x/\text{TiO}_2$ -CNTs (Sg) (■), $\text{MnO}_x/\text{TiO}_2$ (Sg) (●), MnO_x/CNTs (◆), $\text{MnO}_x/\text{TiO}_2$ -CNTs (St) (▲) and $\text{MnO}_x/\text{TiO}_2$ (St) (▼). (Right one)

3.4. Catalytic activity characterization

CB conversion activity and turnover frequency (TOF) of the catalysts were presented in Fig. 4. The catalysts containing CNTs showed higher CB removal efficiencies in low-temperature region and had higher TOF. The CB conversions for $\text{MnO}_x/\text{TiO}_2$ in the studied temperature range were always lower than those for $\text{MnO}_x/\text{TiO}_2$ -CNTs prepared by the same method, and it is the same with TOF. Particularly for $\text{MnO}_x/\text{TiO}_2$ -CNTs (Sg), the removal efficiency of CB reached 95.0% at a reaction temperature as low as 150°C, and it has the highest activity and TOF among the five catalysts. At a reaction temperature of 250°C, CB removal efficiencies of all catalysts reached more than 95%. These results suggested that the introduction of CNTs into the catalysts promotes the catalytic activity for CB oxidation in low-temperature region. Moreover, no activity decrease was observed in all of our CNTs-containing samples for more than 150 hours tests.

Although the mechanism of CB oxidation promoted by CNTs is still not yet understood and needs to be further clarified, the synergetic effect of CNTs on the activity of the composite catalysts is considered, and several reasons for this synergy can be mentioned. Firstly, CNTs with higher specific surface acting as dispersing agent may prevent agglomeration of TiO_2 and MnO_x , thus providing a high active surface area of the resulting composite catalysts, as seen from BET results. In fact, the crystal size of particles in the samples with CNTs was smaller than those without CNTs. Additionally, the effect is also possibly promoted by selective adsorption of CB on the surface of CNTs. Recently, it was reported that

CB molecules can be selectively adsorbed by CNTs through π -electron coupling between the flat surfaces of CB and CNTs [13, 25]. In our experiments, $\text{MnO}_x/\text{TiO}_2$ nanoparticles were partly coated on the CNTs evenly. When a CB molecule was adsorbed on the free surface of CNTs, it was possible to be nucleophilically attacked by the neighboring MnO_x , which promoted the catalytic oxidation of CB at a low temperature [26, 27].

Acknowledgement: This work was supported by the United Nations Industrial Development Organization (UNIDO) (Project No. TF/CPR/03/006), the National Foundation of Zhejiang Province, China (Grant No. Z4080070), and the Foundation of Science and Technology Bureau of Zhejiang Province, China (Grant Nos. 2008C21057 and 2009C34003).

References:

- [1] A. A. Meharg, D. Osborn, *Nature* 375 (1995) 353-354.
- [2] A. Musialik-Piotrowska, K. Syczewska, *Catal Today*, 7 (2002) 333-342.
- [3] L. Pinard, J. Mijoin, P. Magnoux, M. Guisnet, *J. Catal.* 215 (2003) 234-244.
- [4] D. Kiessling, R. Schneider, P. Kraak, M. Haftendorn, G. Wendt, *Appl. Catal. B* 19 (1998) 143-151.
- [5] R. Schneider, D. Kiessling, G. Wendt, *Appl. Catal. B* 28 (2000) 187-195.
- [6] E. Kantzer, D. Dobber, D. Kiessling, G. Wendt, *Stud Surf Sci Catal*, 143 (2002) 489-497.
- [7] I. M. Freidel, A. C. Frost, K. J. Herbert, F.S. Meyer, J. C. Summers, *Catal. Today* 17 (1993) 367-382.
- [8] B. Mendyka, A. Musialik-Piotrowska, K. Syczewska, *Catal. Today* 11 (1992) 597-610.
- [9] P. Subbanna, H. Greene, F. Desal, *Environ. Sci. Technol.* 22 (1988) 557-561.
- [10] R. Weber, T. Sakurai, H. Hagenmaier, *Appl. Catal. B* 20 (1999) 249-256.
- [11] P. Serp, M. Corrias, P. Kalck, *Appl. Catal. A*, 253 (2003) 337-358.
- [12] R. Q. Long, R. T. Yang, *J. Am. Chem. Soc.* 123 (2001) 2058-2059.
- [13] W. Chen, L. Duan, D. Q. Zhu, *Environ. Sci. Technol.* 41 (2007) 8295-8300.
- [14] P. Vincent, A. Brioude, C. Journet, S. Rabaste, S.T. Purcell, J.L. Brusq, J.C. Plenet, *J. Non-Cryst. Solids*, 311 (2002) 130-137.
- [15] A. Jitianu, T. Cacciaguerra, R. Benoit, S. Delpeux, F. Beguin, S. Bonnamy, *Carbon* 42 (2004) 1147-1151.
- [16] Y. Li, X. B. Zhang, X. Y. Tao, J. M. Xu, F. Chen, L. H. Shen, X. F. Yang, F. Liu, G. Van Tendeloo, H. J. Geise, *Carbon* 43 (2005) 1325-1328.
- [17] X. P. Huang, C. X. Pan, X. T. Huang, *Mater. Lett.* 61 (2007) 934-936.
- [18] M. Baldi, V.S. Escribano, J.M.G. Amores, F. Milella, G. Busca, *Appl. Catal. B* 17 (1998) 175-182.
- [19] J. M. Gallardo-Amores, T. Armadori, G. Ramis, E. Finocchio, G. Busca, *Appl. Catal. B* 22 (1999) 249-259.
- [20] Y. Yao, G.H. Li, S. Cistion, R.M. Lueptow, K.A. Gary, *Environ. Sci. Technol.* 42 (2008) 4952-4957.
- [21] X. Y. Wang, Q. Kang, D. Li, *Catal. Commun.* 9 (2008) 2158-2162.
- [22] F. Kapteijn, L. Singoredjo, A. Andreini, J. A. Moulijn, *Appl. Catal. B* 3 (1994) 173-189.
- [23] F. Arena, T. Torre, C. Raimondo, A. Parmaliana, *Phys. Chem. Chem. Phys.* 3 (2001) 1911-1917.
- [24] J. Carno, M. Ferrandon, E. Bjornbom, S. Jaras, *Appl. Catal. A* 155 (1997) 265-281.
- [25] D. Q. Yang, B. Hennequin, E. Sacher, *Chem. Mater.* 18 (2006) 5033-5038.
- [26] Y. Liu, Z. B. Wei, Z. C. Feng, M. F. Luo, P. L. Ying, C. Li, *J. Catal.* 202 (2001) 200-204.
- [27] E. Finocchio, G. Busca, M. Notaro, *Appl. Catal. B* 62 (2006) 12-20.